



## Binding partners for curcumin in human schwannoma cells: Biologic Implications

Laura S. Angelo<sup>a,\*</sup>, David S. Maxwell<sup>b,†</sup>, Ji Yuan Wu<sup>a</sup>, Duoli Sun<sup>b</sup>, David H. Hawke<sup>c</sup>, Ian E. McCutcheon<sup>d</sup>, John M. Slopis<sup>e</sup>, Zhenghong Peng<sup>b</sup>, William G. Bornmann<sup>b</sup>, Razelle Kurzrock<sup>a</sup>

<sup>a</sup> Department of Investigational Cancer Therapeutics, (Phase I Program), The University of Texas MD Anderson Cancer Center, Houston, USA

<sup>b</sup> Department of Experimental Therapeutics, The University of Texas MD Anderson Cancer Center, Houston, TX, USA

<sup>c</sup> Proteomics Core Facility, The University of Texas MD Anderson Cancer Center, Houston, TX, USA

<sup>d</sup> Department of Neurosurgery, The University of Texas MD Anderson Cancer Center, Houston, TX, USA

<sup>e</sup> Department of Neuro-Oncology, The University of Texas MD Anderson Cancer Center, Houston, TX, USA

### ARTICLE INFO

#### Article history:

Received 26 September 2012

Revised 29 November 2012

Accepted 6 December 2012

Available online 13 December 2012

#### Keywords:

Curcumin

hsp70

hsp90

D-3-phosphoglycerate dehydrogenase

Biotinylation

### ABSTRACT

Curcumin (diferuloylmethane) is a potent anti-inflammatory and anti-tumorigenic agent that has shown preclinical activity in diverse cancers. Curcumin up-regulates heat shock protein 70 (hsp70) mRNA in several different cancer cell lines. Hsp70 contributes to an escape from the apoptotic effects of curcumin by several different mechanisms including prevention of the release of apoptosis inducing factor from the mitochondria and inhibition of caspases 3 and 9. Previously we showed that the combination of curcumin plus a heat shock protein inhibitor was synergistic in its down-regulation of the proliferation of a human schwannoma cell line (HEI-193) harboring an NF2 mutation, possibly because curcumin up-regulated hsp70, which also binds merlin, the NF2 gene product. In order to determine if curcumin also interacts directly with hsp70 and to discover other binding partners of curcumin, we synthesized biotinylated curcumin (bio-curcumin) and treated HEI-193 schwannoma cells. Cell lysates were prepared and incubated with avidin-coated beads. Peptides pulled down from this reaction were sequenced and it was determined that biotinylated curcumin bound hsp70, hsp90, 3-phosphoglycerate dehydrogenase, and a  $\beta$ -actin variant. These binding partners may serve to further elucidate the underlying mechanisms of curcumin's actions.

© 2012 Published by Elsevier Ltd.

### 1. Introduction

Curcumin (diferuloylmethane) is a potent anti-inflammatory and anti-tumorigenic agent that has shown preclinical activity in several different types of cancer and other diseases including Alzheimer's, Parkinson's, inflammatory bowel disease, psoriasis, and certain infections.<sup>1–5</sup> Tumor regression and stabilization has been reported in a small subset of patients with advanced, refractory pancreatic cancer treated with oral curcumin.<sup>6</sup> However, curcumin can also act as a double-edged sword in that it has both anti-oxidant and pro-oxidant properties and its actions and effects depend on the disease, the concentration of curcumin ingested, and the host's immune system. The list of known molecular targets of cur-

Abbreviations: Hsp, Heat shock protein; PGDH, 3-phosphoglycerate dehydrogenase.

\* Corresponding author. Address: Department of Investigational Cancer Therapeutics, M D Anderson Cancer Center, Unit 455, Houston, TX 77030, USA. Tel.: +1 713 792 7736; fax: +1 713 563 0566.

E-mail address: [lsangelo39@gmail.com](mailto:lsangelo39@gmail.com) (L.S. Angelo).

† These authors contributed equally to this work.

cumin is extensive, continues to evolve, and includes growth modulators, transcription factors, cell signaling molecules, adhesion molecules, and tumor suppressor and apoptosis genes. Specific examples of curcumin's molecular effects include inhibition of NF- $\kappa$ B, up-regulation of caspases 3 and 8, inhibition of the Akt/mTOR pathway, decreased COX-2 expression via the TNF- $\alpha$  receptor, down-regulation of *Bcl-2*, and up-regulation of *Bax*.<sup>1</sup> Some of these targeted genes are particularly important in cancer and inflammation, and demonstrate curcumin's ability to affect cell survival and apoptosis pathways in many different cell types.

Curcumin also up-regulates heat shock protein 70 (hsp70) mRNA as a means of escape from the apoptotic effects of this compound.<sup>7–9</sup> We previously showed that the combination of curcumin and a heat shock protein inhibitor (KNK437) had profound inhibitory effects on the growth of a human schwannoma cell line (HEI-193) that contains a loss of heterozygosity of one allele and a mutation of the other allele of the neurofibromatosis 2 (*NF2*) gene.<sup>10</sup> We also demonstrated that merlin, the protein product of the *NF2* gene, interacted with hsp70 at the protein level.<sup>10</sup> Curcumin also up-regulated hsp70 mRNA in HEI-193 cells. These results led us to examine what the protein targets or binding partners of

curcumin are in curcumin-treated schwannoma cells, and what the nature of these interactions is on the molecular level.

## 2. Materials and methods

### 2.1. Formulation of biotinylated curcumin

Briefly, to the mixture of curcumin (94%) (110 mg, 0.28 mmol), Biotin (157 mg, 0.28 mmol), DMAP (60 mg, 0.49 mmol) and EDC (130 mg, 0.84 mmol), was added 21 ml DMF (anh.). The reaction solution was heated to 50 °C overnight. The solvent was removed under vacuum at 50 °C. After cooling down, the residual was dissolved in 10 ml DCM, 10 g silica gel was added. The crude product was purified over silica gel with ethyl acetate (curcumin was obtained about 10 mg) ethyl acetate/methanol 1:1 and then methanol. The methanol washing liquor was further purified with HPLC to obtained the 1:1 adduct as the final product (30 mg yield 13%, Purity >98% by HPLC). See [Supplementary data and Supplementary Figures S1–S5](#) for a complete description.

### 2.2. Cell line

HEI-193 schwannoma cells were a generous gift of the House Ear Institute (Los Angeles, CA) and contain a loss of heterozygosity and a point mutation in the neurofibromatosis 2 (*NF2*) gene (described previously.<sup>10–12</sup> Cells were maintained in DMEM-F12 media plus 10% fetal bovine serum (GIBCO/BRL, Carlsbad, CA) at 37 °C and 5% CO<sub>2</sub>.

### 2.3. Reagents

MTT (3-(4,5-dimethylthiazol-2-yl)-2,5-diphenyltetrazolium bromide) and curcumin were purchased from Sigma (St. Louis, MO). MTT stock solution was prepared as 5 mg/ml in sterile PBS. Curcumin and biotinylated curcumin stock solutions were 100 mM in DMSO. Silver SNAP stain for mass spectrometry was purchased from Thermo Scientific (Waltham, MA). Anti-hsp70 antibody was purchased from Santa Cruz (Santa Cruz, CA).

### 2.4. MTT (3-(4,5-dimethylthiazol-2-yl)-2,5-diphenyltetrazolium bromide) assay

In order to determine the growth response of HEI-193 cells to curcumin or biotinylated curcumin,  $5 \times 10^3$  HEI-193 cells were plated in triplicate wells of a 96 well plate. MTT assay was performed as described by the manufacturer's instructions. Cells were  $\geq 99\%$  viable for all experiments. Briefly, cells were allowed to adhere overnight after plating, and then treated with or without curcumin or biotinylated curcumin at various concentrations. After 72 h of incubation, the cells were lysed per MTT assay protocol. The 96 well plate was read at an optical density (OD) of 570 (M2 plate reader, Molecular Devices, (Sunnyvale, California). Statistical analysis was carried out by SoftMax pro 4.1. Percent growth inhibition was calculated using 0.1% dimethyl sulfoxide (DMSO) treated cells as a control for 100% growth. Data are expressed as the mean  $\pm$  standard deviation (SD) (Graph Pad 5 software, La Jolla, CA).

### 2.5. Identification of hsp70 in cell lysates

To determine which protein band in the treated cell lysates was hsp70,  $1.2 \times 10^6$  HEI-193 cells were grown in 10 cm dishes overnight until 80% confluent. Cells were then treated with 100  $\mu$ M bio-curcumin for 30 min. Cells were washed twice with  $1 \times$  PBS

(4 °C) and lysed on ice with buffer containing 1% triton-X 100, 10 mM Tris-HCl, 1 mM EDTA, 1 mM EGTA, 1 mM sodium pyruvate, 1 mM sodium vanadate, 1 mM PMSF, 1  $\mu$ M leupeptin, 10  $\mu$ g/ml aprotinin, 0.5% sodium deoxycholate, and 20% glycerol, pH 7.2. Protein concentration was measured by the BCA (bicinchoninic acid) protein assay (Pierce, Waltham, MA). Twenty micrograms of protein lysate was loaded onto 8% SDS-PAGE gels. Gels were either silver stained or immuno-blotted with anti-hsp70 antibody for comparison.

### 2.6. Affinity purification of curcumin binding proteins

For purification of proteins binding the bio-curcumin, 1 mg/ml of curcumin-treated HEI-193 cell protein lysate was incubated with NeutraAvidin beads (Pierce) (4 °C for 1 h). Different incubation times were tested to determine optimal binding conditions of targeted proteins and Avidin beads. Precipitates were washed 4 times with wash buffer containing 10 mM Tris-HCl, 1% triton-X100, 1 mM sodium vanadate and 1 mM PMSF. Gels were subjected to silver staining per manufacturer's instructions (Pierce). Specific strong bands appearing on the gel and also those near 70 kD after silver staining were cut out, digested with trypsin, and sent to the RPPA/functional proteomics core lab at MD Anderson for mass spectrometry analysis (LTQ, Thermo Scientific, Waltham, MA). Peptide sequences were analyzed using NCBI's non-redundant protein database (Mascot software, Noida, UP, India).

### 2.7. In silico analysis of binding interactions

#### 2.7.1. General computational

Peptide sequences identified by Mascot software as binding to bio-curcumin in HEI-193 cells were further analyzed to determine potential molecular binding sites of the bio-curcumin to the proteins identified. Protein structures were analyzed on a 4-quad core (16-core) 2.4 Ghz AMD Opteron system using the RHEL 5.x OS and molecular modeling software, Sybyl-X (Tripos, Inc, St. Louis, MO) and Schrödinger Suite 2011 (Schrödinger LLC, New York, NY). Docking was completed with both Surflex V2.510.11089<sup>13</sup> and Glide version 5.5 (Schrödinger, LLC). Several SPL (SPL programming language) scripts were utilized as part of the searching and analysis.

#### 2.7.2. Virtual ligand preparation

Curcumin was prepared as the enol-keto tautomer in Chemdraw on the PC since this is the preferred form as shown by high level quantum chemical calculations.<sup>14</sup> The structure was saved out as a mol file, transferred to the Linux box, and converted to an SDF formatted file. To prepare curcumin for the Glide docking calculation, the molecule was read into Maestro, a LigPrep calculation was done to generate a 3D structure, which was followed by an Epik Version 2.2 (Schrödinger, LLC) calculation to obtain correctly ionized structures with alternative tautomeric states. This preparation resulted in both the enol-keto and diketo states. For docking with Surflex, the structure was read using Unity Translate, modified to match the two tautomeric forms, and then Concord<sup>15</sup> was utilized to prepare a suitable 3D structure.

To prepare the structure for docking with Surflex, the hsp90 crystal structure was read into Sybyl and the geldanamycin structure was extracted out and saved separately. The full structure was then minimized to a gradient of 0.05 kcal/(mol Å) with the Powell method using the MMFF94 force field with non-bonded cutoff of 12 Å and distant dependent dielectric of 2.0. To prepare for Glide docking, a LigPrep calculation was completed on the structure.

### 2.7.3. Preparation and docking in hsp70 structure using Glide/vsw

The Protein Data Bank (PDB) structure 2e8a was read into Maestro Version 9.2 (Schrödinger, LLC, 2011) and a protein preparation was completed with default options, except that missing side chains were generated and all waters were kept. This was followed by a heteroatom states calculation, then an H-bond assignment. An Impref minimization of hydrogens only in the structures was done, which was followed by an Impref minimization of all atoms to RMSD = 0.5 Å. The same setup and minimization was completed with crystal waters removed. A Sitemap Version 2.5 (Schrödinger, LLC) calculation was completed on the relaxed structure without waters. A Glide Grid calculation was completed on the prepared hsp70 structure using the crystal ligand, AMP-PNP, as the basis for defining the box. The two tautomeric forms of curcumin were docked into the hsp70 structures with and without water using the Virtual Screening Workflow. No constraints were utilized during the docking calculations.

### 2.7.4. Preparation and docking in hsp70 structure using Surflex-Dock

The structure 2e8a was read into Sybyl and all bonds to the  $Mg^{2+}$  atom were removed. A protein preparation was completed to charge the termini and add hydrogen atoms. Lone pairs that were created during the hydrogen addition stage were removed and  $Mg^{2+}$  was changed to  $Ca^{2+}$  to avoid issues during minimization with the MMFF94 force field. All waters in the structure were kept. A staged minimization was used to optimize the structure and this consisted of 250 steps each for hydrogens, waters, hydrogens + side chains, hydrogens + side chains + backbone except  $C\alpha$ , ligand, and all atoms. The Powell minimization method was utilized with initial Simplex optimization. The MMFF94 force field was selected and a non-bonded cutoff of 12 Å was applied. A distance dependent dielectric of 2.0 was used to further screen the electrostatic interactions. The same setup and minimization was completed with crystal waters retained. The protocol was defined based on the AMP-PNP ligand.

### 2.7.5. Preparation and docking in D-3-phosphoglycerate dehydrogenase structure using Surflex-Dock and Glide/vsw

Preparation and docking of D-3-phosphoglycerate dehydrogenase based on PDB structure 2g76 with and without crystal waters was completed in the same manner as hsp70.

### 2.7.6. Preparation and docking in hsp90 structure using Surflex-Dock and Glide/vsw

Preparation and docking of hsp90 based on PDB structure 1yet with and without crystal waters was completed in the same manner as hsp70.

## 3. Results

### 3.1. Synthesis of biotinylated curcumin

A structural formula of the synthesized biotinylated curcumin is shown in Fig. 1. Details regarding the synthesis and characterization of biotinylated curcumin are available in the [Supplementary Materials and Methods](#) and [Supplementary Figures S1–S5](#).

### 3.2. Biotinylated curcumin inhibits proliferation of HEI-193 cells

HEI-193 cells were incubated with increasing concentrations of curcumin or bio-curcumin for 72 h. The  $IC_{50}$  for curcumin was 18  $\mu M$ ; the  $IC_{50}$  for bio-curcumin was 36  $\mu M$  (Fig. 2). These results

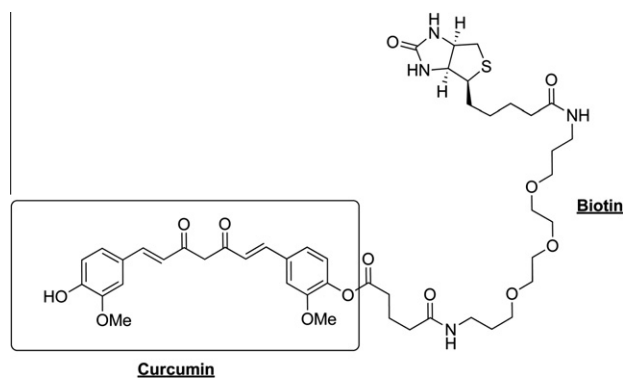


**Figure 1.** Structure of biotinylated curcumin with curcumin fragment highlighted.

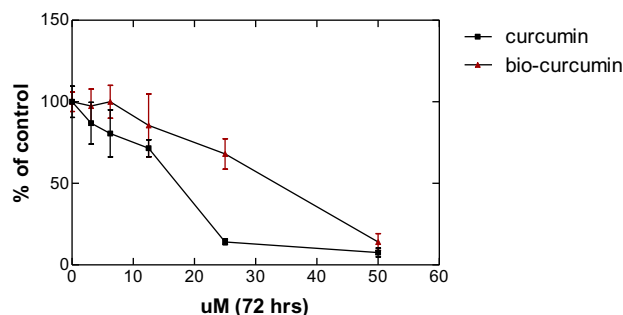


**Figure 2.** Biotinylated curcumin (bio-curcumin) is less effective ( $IC_{50}$  = 36  $\mu M$ ) at inhibiting the proliferation of HEI-193 cells than curcumin ( $IC_{50}$  = 18  $\mu M$ ).  $5 \times 10^3$  HEI-193 cells were plated in triplicate wells of a 96 well plate and treated with 0–50  $\mu M$  of curcumin or bio-curcumin for 72 h. MTT assay was performed. Results shown are the mean and standard deviation of three experiments.

indicate that the biotinylated compound could effectively inhibit the target cell line, albeit at higher concentrations than needed for the parental compound.

### 3.3. Purification of binding partners for biotinylated curcumin

HEI-193 cells were incubated with curcumin or biotinylated curcumin for 30 min, and cell lysates were incubated with avidin beads for 1, 2, or 16 h at 4 °C. Various times of incubation were tested in order to optimize binding conditions (Fig. 3). Two hours was found to be optimal. Lysates were run on two different 8% SDS–PAGE gels. The gel was silver-stained to see the protein bands, and six bands were chosen for purification based on these experiments (Fig. 3, right panel). These six bands were cut from the gel, digested with trypsin, and sent to MD Anderson's core proteomics lab for analysis by mass spectrometry. Peptide sequences were obtained and analytical software was used to determine candidate proteins (Mascot software). Table 1 lists four of the most prominent proteins that were found to interact with biotinylated curcumin in HEI-193 cells: hsp70, hsp90, 3-phosphoglycerate dehydrogenase, and  $\beta$ -actin (arrows, Fig. 3). For a complete list of all of the protein fragments that were pulled down with biotinylated curcumin see [Supplementary Table S1](#).

Interestingly, both hsp70 and hsp90 were found to be binding partners of bio-curcumin. 3-phosphoglycerate dehydrogenase and  $\beta$ -actin were also on the list of human proteins that interacted with bio-curcumin. We chose to look at potential docking sites for bio-curcumin in hsp70, hsp90, and 3-phosphoglycerate dehydrogenase since curcumin influences the expression and function of both hsp70 and hsp90, and 3-PGDH is a newly discovered binding

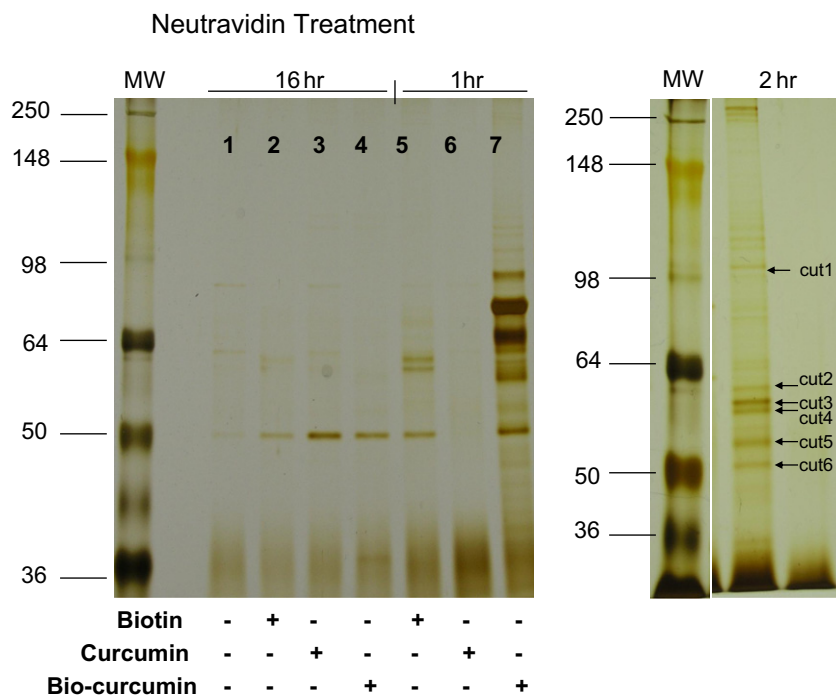


**Figure 3.** For purification of proteins binding to bio-curcumin, 1 mg/ml of curcumin-treated HEI-193 cell protein lysate was incubated with NeutraAvidin beads for 2 h at 4 °C. Beads were washed 4 times and loaded onto 8% SDS PAGE gels. Gels were subjected to silver stain. Optimization of the incubation period with Neutraavidin beads (1 and 16 hour incubation times) is shown in the left-hand panel. Two hours proved to be the optimal incubation for interaction of the beads with bio-curcumin bound proteins (right-hand panel). The most prominent specific bands were chosen for further analysis by cutting the bands from the gel, treating them with trypsin, and sequencing them (cuts 1–6). Cut 1 contained hsp90, cut2 contained hsp70, and cut 3 contained  $\beta$ -actin and 3-PGDH. MW = molecular weight marker; Lane 1 = bands pulled down with bio-curcumin; lane 2 = beads alone. Other non-relevant lanes were cut from the photo for ease of understanding.

partner of curcumin. Since a high resolution X-ray crystal structure of  $\beta$ -actin could not be found, docking of curcumin to that structure was not included in the analysis. We further analyzed the specific residues involved in the binding of these three human proteins to bio-curcumin.

### 3.4. Docking of curcumin in hsp70

Determination of the most likely location for binding was done by running a Sitemap calculation (non-covalent binding), which

resulted in five sites with scores of 1.02, 1.00, 0.67, 0.60, and 0.56. Authors of the program state that a site score threshold of 0.80 can clearly distinguish between good and poor sites, thus only the first two should be considered. The first site corresponds to the ATPase binding site and the second is on the backside of that site. Since docking of bio-curcumin would be difficult due to the long flexible chain, it was docked as unlabeled curcumin in two tautomeric forms. Docking to the ATPase site was completed with two different docking programs with and without crystal waters (see Table 1). For Surflex-Dock, the hsp70 structure without water

**Table 1**

Receptor	Form	Crystal Water			No Water		
		Surflex	XP Glide Score	Prime MM-GBSA	Surflex	XP Glide Score	Prime MM-GBSA
HSP-70	EK	2.46	-10.15	-29.65	11.44 <sup>b</sup>	-2.61	-49.24
	DK	7.79	-9.44	-57.67	11.14	-8.26	-57.94
HSP-90	EK	7.70	-5.77	-39.93	6.17	-5.48	-72.45 <sup>b</sup>
	DK	7.87	-6.31	-54.46	7.48	-5.06	-57.50
3-Phospho Glycerate Dehydrogenase	EK	10.16	-8.32	-61.40	8.04 <sup>b</sup>	-7.81	-71.66
	DK	9.91	-7.19	-54.15	7.83	-6.88	-83.93
Beta actin	ND	ND	ND	ND	ND	ND	ND

<sup>a</sup> Cells are colored from green–yellow–red, signifying better-to-worse scoring; EK—enol-keto, DK—diketo.

<sup>b</sup> Configuration selected for ligand-receptor images. ND—not done.



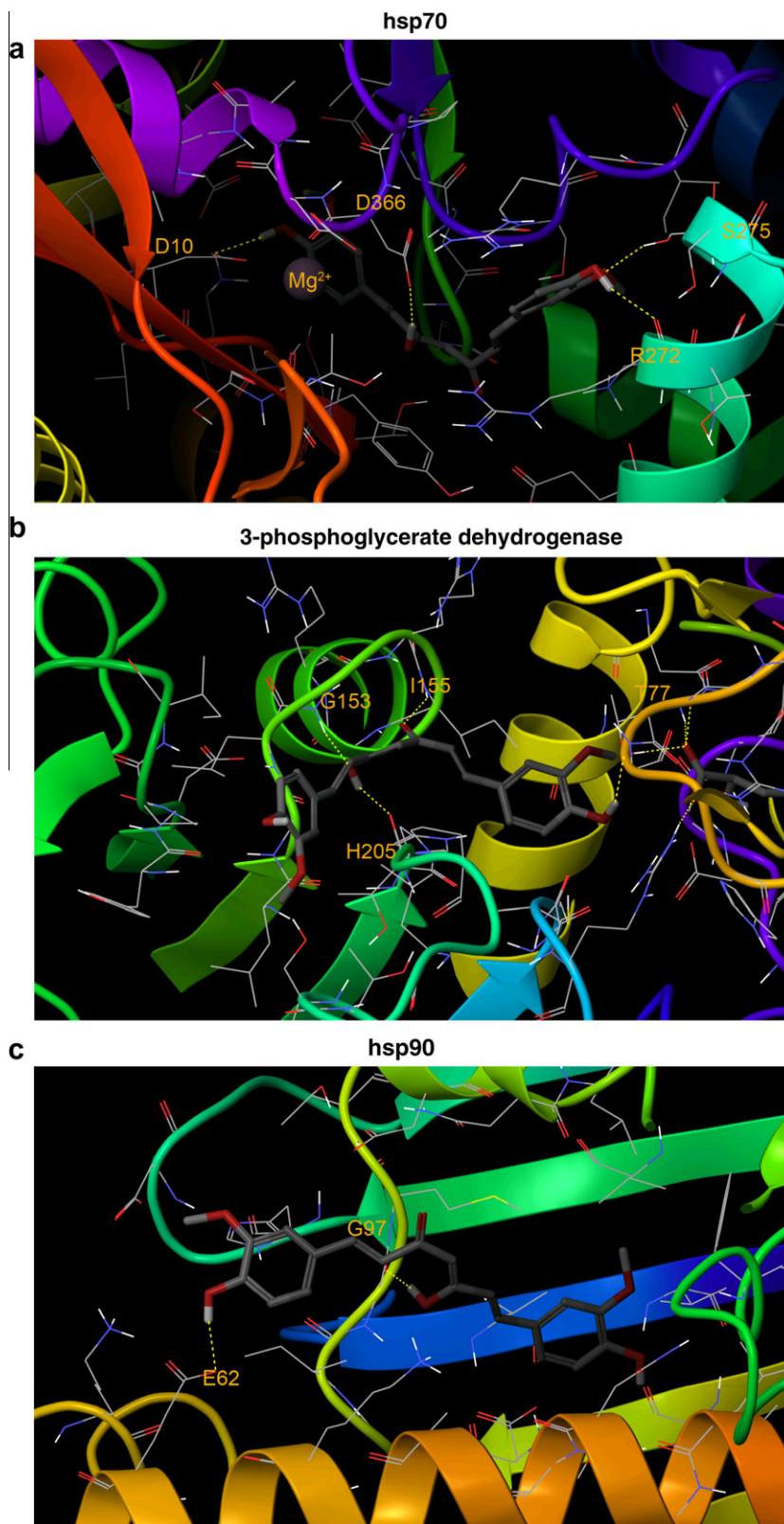


**Figure 4.** (a) View of ATPase site of hsp70 with proposed orientation of curcumin obtained from docking with Surflex. One end of curcumin interacts in an H-bond with the side chain of D10, whereas the other end interacts with the side chain of S275 and backbone of R272. The hydroxyl group in the middle of curcumin interacts with the side chains of D366 and T37. (b) View of the proposed orientation of curcumin in NAD binding site of 3-PGDH. One end of the curcumin interacts in an H-bond with the side-chain of T77 whereas the other end is open for attachment of the biotin label. The hydroxyl group in the middle of curcumin interacts with the backbone amide of G153 and carbonyl of H205. (c) View of geldanamycin binding site in hsp90 with proposed orientation of curcumin obtained from docking with Glide/vsw. One end interacts in an H-bond with E62 and the middle hydroxyl group interacts with the backbone of G97. In each case, the enol-keto form of curcumin was docked into the protein structure without water. Images were created with Maestro version 9.2

was preferred and the lower scores with water are attributable to the significant crash values, which signify inappropriate penetration of the curcumin into the protein. There is only a slight difference in the scoring for the two forms of curcumin, with a preference for enol-keto (EK) form over the diketo (DK) form. In

the hsp70 structure without water (see Fig. 4a), curcumin interacts through an H-bond with Asp10, whereas the other end H-bonds with the side chain of Ser275 and the backbone carbonyl of Arg272. The hydroxyl in the middle of the structure interacts with the side-chain of Asp366. Importantly, the area around Ser275/

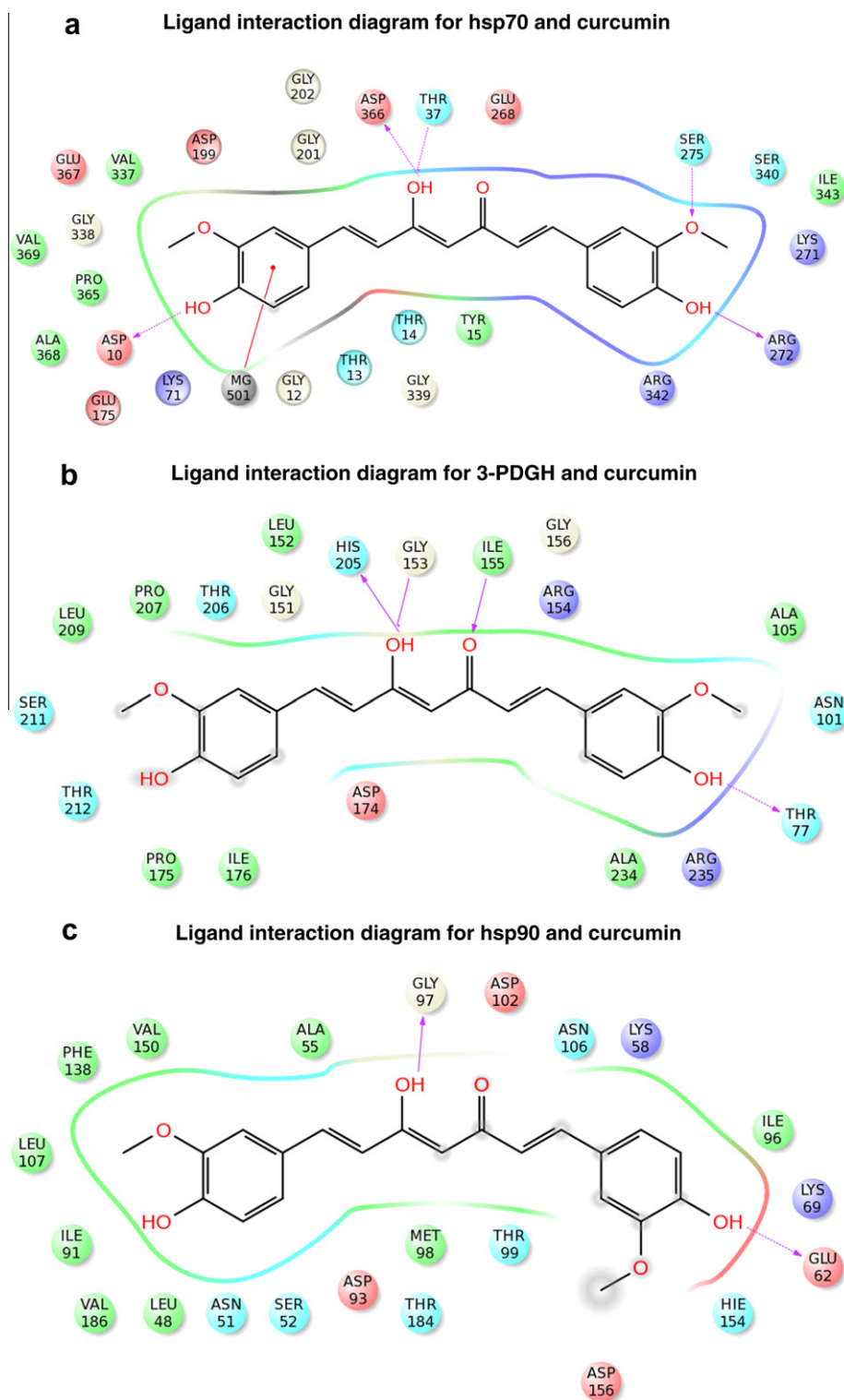


**Fig. 5.** a. Ligand interaction diagram for hsp70 and curcumin. (b) Ligand interaction diagram for 3-PDGH and curcumin (c). Ligand interaction diagram for hsp90 and curcumin. Residue coloring is as follows: Acidic residues are red, hydrophobic residues are green, basic residues are purple, polar residues are blue, other residues are light gray, and metal atoms are darker gray. Solid pink lines designate H-bonds to the protein backbone and dotted pink lines designate H-bonds to protein side chains. The colored line surrounding the ligand represents the protein pocket and gaps in the line designate opening of the pocket. Other details may be found in the Maestro 9.3 manual. Images were created with Maestro version 9.3.

Arg272 appears to be open for attachment of the biotin. For calculations with the Schrödinger software, the XP Glide score shows a preference for the receptor structure having crystal waters. Without the water, docking of curcumin led to the unexpected preference of the diketo (DK) form using both scoring functions.

### 3.5. Docking of curcumin in D-3-phosphoglycerate dehydrogenase

The Sitemap calculation on this structure resulted in five sites with scores of 1.06, 0.98, 0.98, 0.81, and 0.73. The first site (1.06) corresponds to the nicotinamide-adenine-dinucleotide (NAD) binding site. The second (0.984) and third sites are adjacent to this site and to the equivalent site in the dimer. We completed docking to the NAD binding site both with and without water. With Surflex-Dock, the structure with crystal waters was favored, and in both cases, there was only a slight difference between the scores for the two tautomeric forms. In the docking configuration without waters, one end of the curcumin interacts in an H-bond (Fig. 4b) with the side-chain of Thr77 whereas the other end is open for attachment of the biotin label. The hydroxyl group in the middle of curcumin interacts with the backbone amide hydrogen of Gly153 and carbonyl of His205. For calculations with the Schrödinger software, the XP Glide score shows a slight preference for the receptor structure with crystal waters and a slight preference for the EK form. However, using the Prime MM-GBSA re-scoring, the preferred form was the DK form in the structure with no water.

### 3.6. Docking of curcumin in hsp90

A Sitemap calculation was not performed on the hsp90 structure and docking was only attempted to the site where geldanamycin is known to bind.<sup>16</sup> Scores for the majority of docking combinations were lower in comparison to the other receptors, especially for Surflex-Dock. The exception was the enol-keto form docked with Glide and rescored with Prime MM-GBSA in the structure with no water. In this configuration, curcumin only formed two H-bonds, one with the backbone carbonyl of Gly97 and another to the Glu62 side-chain (Fig. 4c). For comparison, geldanamycin scored 13.36 with Surflex-Dock, −5.26 with Glide-XP, and −78.12 with Prime MM-GBSA. With Surflex-Dock and Prime MM-GBSA scoring, geldanamycin scored higher than curcumin. It is interesting to note that although a fluorescence polarization study shows that curcumin competes for geldanamycin, it does so weakly at 6.2  $\mu\text{M}$ .<sup>17</sup> Schematic diagrams of the proposed interaction of curcumin with hsp70, 3-PDGH, and hsp90 are shown in Figures 5a, b, and c, respectively.

## 4. Discussion

Curcumin is a natural compound that has shown efficacy and low toxicity in several types of cancer. Our previous work demonstrated that curcumin up-regulates hsp70 in human schwannoma cells<sup>10</sup> and also inhibits the growth of these cells. These observations prompted us to explore which proteins curcumin targets/binds to inside schwannoma cells in order to elicit its effects on proliferative and other pathways. We used biotinylated curcumin (bio-curcumin) as a probe to identify protein targets of curcumin in schwannoma cells. A 2 h incubation time with biotinylated curcumin proved to be optimal for the binding experiments. The 16 hour incubation time resulted in suboptimal bands (Fig. 3). This may partially be due to curcumin's ability to ubiquitinate many proteins and target them for degradation by the proteasome.<sup>18</sup> Hence, longer incubation times resulted in fewer bands on the gel. Interestingly, we found that curcumin binds to hsp70, hsp90,

and 3-phosphoglycerate dehydrogenase (PGDH). While binding of curcumin to hsp90 has been published,<sup>19</sup> binding to hsp70 and 3-PGDH has not. Molecular docking and site mapping software was used to select potential binding sites and propose interactions of bio-curcumin to these three proteins.

Using a series of molecular protein docking software programs, we were able to predict with some accuracy where bio-curcumin may be binding each of the three proteins we analyzed. Hsp70 is up-regulated by curcumin at the mRNA and protein levels in many cell types,<sup>7–10</sup> while a decrease in hsp70 degradation is also a possible mechanism of hsp70 up-regulation. The SiteMap calculation performed indicated that bio-curcumin binds hsp70 at the ATPase binding site and also at a second binding site on the backside of the ATPase binding site. Because of the high docking scores generated for this site, we are confident that curcumin is binding this site, but cannot exclude other sites of interaction that we did not pick up in our analysis. The ATPase activity in the nucleotide binding domain of hsp70 functions to regulate the turnover of target proteins in the substrate binding domain. These two domains function through an inter-domain allosteric mechanism. Hence, when ATP is bound, turnover of proteins bound to the substrate binding domain is rapid. Hydrolysis of ATP to ADP slows down this on-off rate and enhances the affinity of hsp70 for the substrate. This communication works both ways in that interaction between the substrate binding domain and its substrates increases the rate of ATP hydrolysis in the nucleotide binding domain.<sup>20,21</sup> Binding of curcumin to the ATPase binding site may change the turnover rate of target proteins that bind and release from hsp70, and thus affect both the half-life and function of these proteins. Since hsp70 has been shown to interact with many proteins involved in cell proliferation and apoptosis,<sup>21</sup> curcumin may affect these pathways by interfering with the normal function of hsp70 in the cells as an escape pathway, and induce cell death.

Hsp90, another molecular chaperone, is involved in the correct folding, function, and stability of many client proteins,<sup>19,22</sup> including molecules important in the control of cell cycle, growth, and apoptosis, and may play a role in malignant transformation. Hsp90 inhibitors are currently being studied as chemotherapeutic agents in the clinic.<sup>23,24</sup> Curcumin has previously been shown to deplete p210 bcr/abl levels in CML cells by directly interacting with hsp90 and disrupting its chaperone function.<sup>19</sup> Hsp90 also bound bio-curcumin in HEI-193 cells. Unfortunately, we were not able to perform a SiteMap calculation on the hsp90 structure because only part of the structure was available for analysis. Therefore docking was only attempted to the site where geldanamycin is known to bind.<sup>15,16</sup> Curcumin competes only weakly for the geldanamycin binding site. None of the sites that came up as possible docking sites for bio-curcumin were known ubiquitination sites for hsp90 or for hsp70 (all lysines), indicating that bio-curcumin is not inhibiting the ubiquitination of hsp70 or hsp90 that might normally target them for degradation.<sup>25</sup> Hence, the increase in hsp70 seen in schwannoma cells<sup>10</sup> is probably not due to a lack of ubiquitination and degradation of hsp70 following curcumin treatment. Curcumin may have opposite effects on hsp70 and hsp90 as demonstrated by the increase of bcr/abl hsp70 complexes in K562 cells and the decrease in bcr/abl hsp90 complexes following curcumin treatment.<sup>19</sup>

The third protein analyzed for interaction with bio-curcumin is 3-phosphoglycerate dehydrogenase (PGDH). PGDH catalyzes the transition of 3-phosphoglycerate into 3-phosphohydroxypyruvate, which is the first and rate-limiting step in the phosphorylated pathway of serine biosynthesis, using NAD<sup>+</sup>/NADH as a cofactor. The Sitemap calculation predicts binding of bio-curcumin to the nicotinamide-adenine-dinucleotide (NAD) binding site. The second and third sites are adjacent to this site and to the equivalent site in the dimer. The NAD binding site is important for the enzyme



activity of PGDH as demonstrated by mutation of this region in individuals with PGDH deficiency.<sup>26</sup> If curcumin is binding in this region, it could interfere with the normal enzymatic activity of PGDH. Certain breast cancers are dependent on serine pathway flux caused by the overexpression of PGDH.<sup>27</sup> Higher grade breast cancers and those that are estrogen receptor negative express the highest levels of PGDH.<sup>27</sup> Inhibition of PGDH with siRNA or shRNA in these high-PGDH expressing breast cancer cell lines results in decreased proliferation. Alternatively, the MCF-7 breast cancer cell line expresses low baseline levels of PGDH.<sup>27</sup> Curcumin up-regulates PGDH in the MCF-7 breast cancer cell line, resulting in increased apoptosis.<sup>28</sup> Hence, curcumin up-regulates PGDH in MCF-7 cells, but this up-regulation results in increased apoptosis, which is in contrast to the breast cancer cell lines that express high baseline levels of PGDH. This may be partially explained by experiments that demonstrate that an increase in PGDH expression also promotes apoptosis in retinal Muller cells.<sup>29</sup> Hence, curcumin treatment may have various effects in a given cell line depending on baseline levels of PGDH or other proteins bound by curcumin.

As mentioned above, curcumin can have both pro-oxidant and anti-oxidant effects. The functional outcome of curcumin treatment on a particular cell type may be concentration dependent, and may also depend on how different proteins functionally respond to high or low concentrations of curcumin. For example, in keratinocytes, lower concentrations of curcumin (1  $\mu$ M) increase chymotrypsin-like activity, whereas higher concentrations (10  $\mu$ M) are inhibitory.<sup>30</sup> In addition, hsp70 and hsp90 show increased expression with concentrations of up to 10  $\mu$ M, while the small hsp27 was unaffected at concentrations 0.3–1  $\mu$ M, but decreased by 34% at 10  $\mu$ M.

One of the roadblocks to effectively treating patients with curcumin in the clinic is the absorption of curcumin by the target cells. Different forms of curcumin, including liposomal curcumin and nano-curcumin, are currently being tested in phase I trials (clinical trials.gov #NCT01403545). Preclinical studies have shown that these forms of curcumin have a longer half-life and/or are able to enter the bloodstream at significantly higher concentrations than free curcumin.<sup>31,32</sup> Many binding partners have been shown for curcumin including but not limited to bovine serum albumin,<sup>33</sup> tubulin,<sup>34</sup> myeloid differentiation protein 2 (MD2),<sup>35</sup> prion protein,<sup>36</sup> beta-amyloid,<sup>37</sup> certain metals including lead and cadmium,<sup>38</sup> and DNA and RNA,<sup>39</sup> although this is still controversial.<sup>40</sup> We demonstrate that hsp70, hsp90, and PGDH bind bio-curcumin.  $\beta$ -actin, a key cytoskeletal protein, was also shown to bind to bio-curcumin using our assay, but further analysis of this interaction was not possible because of the absence of a crystal structure for  $\beta$ -actin. Importantly, hsp70, hsp90, and PGDH are all relevant to cancer growth.<sup>8,9,17,19,21,27,28</sup> Binding of these proteins to curcumin may partially explain some of the anti-proliferative/pro-apoptotic effects seen in cancer cells following curcumin treatment. Further study is needed to confirm the binding sites proposed by the in silico analysis and their relationship to curcumin's biologic effects.

## Acknowledgment

This work was funded in part by The Denise Terrill Charity Classics

## Supplementary data

Supplementary data associated with this article can be found, in the online version, at <http://dx.doi.org/10.1016/j.bmc.2012.12.008>.

## References and notes

- Marathe, S. A.; Dasgupta, I.; Prakash, D.; Gnanadhas, D. P.; Chakravorty, D. *Expert Opin. Biol. Ther.* **2011**, *11*, 1485.
- Schaffer, M.; Schaffer, P. M.; Zidana, J.; BarSela, G. *Curr. Opin. Clin. Nutr. Metab. Care* **2011**, *14*, 588.
- Ali, T.; Shakir, F.; Morton, J. *Digestion* **2012**, *85*, 249.
- Mythri, R. B.; Bharath, M. M. *Curr. Pharm. Des.* **2012**, *18*, 91.
- Ye, M.-X.; Li, Y.; Yin, H.; Zhang, J. *Int. J. Mol. Sci.* **2012**, *13*, 3959.
- Dhillon, N.; Aggarwal, B. B.; Newman, R. A.; Wolff, R. A.; Kunnumakkara, A. B.; Abbruzzese, J. L.; Ng, C. S.; Badmaev, V.; Kurzrock, R. *Clin. Cancer Res.* **2008**, *14*, 4491.
- Rashmi, R.; Kumar, S.; Karunakaran, D. *Carcinogenesis* **2004**, *25*, 179.
- Khar, A.; Ali, A. M.; Pardhasaradhi, B. V.; Varalakshmi, C. H.; Anjum, R.; Kumari, A. L. *Cell Stress Chaperones* **2001**, *6*, 368.
- Kato, K.; Ito, H.; Kamei, K.; Iwamoto, I. *Cell Stress Chaperones* **1998**, *3*, 152.
- Angelo, L. S.; Wu, J. Y.; Meng, F.; Sun, M.; Kopetz, S.; McCutcheon, I. E.; Slopis, J. M.; Kurzrock, R. *Mol. Cancer Ther.* **2011**, *10*, 2094.
- Hung, G.; Faudoa, R.; Li, X.; Xeu, Z.; Brackmann, D. E.; Hittselberg, W.; Saleh, E.; Lee, F.; Gutmann, D. H.; Slattery, W.; Rhim, J. S.; Lim, D. *Int. J. Oncol.* **1999**, *14*, 409.
- Hung, G.; Li, X.; Faudoa, R.; Xeu, Z.; Kluwe, L.; Rhim, J. S.; Slattery, W.; Lim, D. *Int. J. Oncol.* **2002**, *20*, 475.
- Jain, A. N. *J. Comput. Aided Mol. Des.* **2007**, *21*, 281.
- Balasubramanian, K. J. *Agric. Food Chem.* **2006**, *54*, 3512; Balasubramanian, K. J. *Agric. Food Chem.* **2006**, *54*, 3512.
- Wei, Y.; Thompson, J.; Floudas, C. A. *Proc. R. Soc. A* **2011**, *468*, 831.
- Stebbins, C. E.; Russo, A. A.; Schneider, C.; Rosen, N.; Hartl, F. U.; Pavletich, N. P. *Cell* **1997**, *89*, 239.
- Giomarelli, C.; Zuco, V.; Favini, E.; Pisano, C.; Dal Piaz, F.; De Tommasi, N.; Zunino, F. *Cell. Mol. Life Sci.* **2010**, *67*, 995.
- Jung, Y.; Xu, W.; Kim, H.; Ha, N.; Neckers, L. *Biochim. Biophys. Acta* **2007**, *1773*, 383.
- Wu, L. X.; Xu, J.-H.; Huang, X.-W.; Zhang, K.-Z.; Wen, C.-X.; Chen, Y.-Z. *Acta Pharmacol. Sin.* **2006**, *27*, 694.
- Mayer, M. P.; Schroder, H.; Rudiger, S.; Paal, K.; Laufen, T.; Bukau, B. *Nat. Struct. Biol.* **2000**, *7*, 586.
- Evans, C. G.; Chang, L.; Gestwicki, J. E. *J. Med. Chem.* **2010**, *53*, 4585.
- Chiosis, G.; Vilenchik, M.; Kim, J.; Solit, D. *Drug Discovery Today* **2004**, *9*, 881.
- Iyer, G.; Morris, M. J.; Rathkopf, D.; Slovin, S. F.; Steers, M.; Larson, S. M.; Schwartz, L. H.; Curley, T.; DeLaCruz, A. Y.; Qe, Q.; Heller, G.; Egorin, M. J.; Ivy, S. P.; Rosen, N.; Scher, H. I.; Solit, D. B. *Cancer Chemother. Pharmacol.* **2012**, *69*, 1089.
- Gartner, E. M.; Silverman, P.; Simon, M.; Flaherty, L.; Abrams, J.; Ivy, P.; Lorusso, P. M. *Breast Cancer Res. Treat.* **2012**, *131*, 933.
- Kundrat, L.; Regan, L. J. *Mol. Biol.* **2010**, *395*, 587.
- Tabatabaie, L.; de Koning, T. J.; Geboers, A. J. J. M.; van den Berg, I. E. T.; Berger, R.; Klomp, L. J. W. *Hum. Mutat.* **2009**, *30*, 749.
- Possemato, R.; Marks, K. M.; Shaul, Y. D.; Pacold, M. E.; Kim, D.; Birsoy, K.; Sethumadhavan, S.; Woo, H.-K.; Jang, H. G.; Jha, A. K.; Chen, W. W.; Barrett, F. G.; Stransky, N.; Tsun, Z. Y.; Cowley, G. S.; Barretina, J.; Kalaany, N. Y.; Hsu, P. P.; Ottina, K.; Chan, A. M.; Yuan, B.; Garraway, L. A.; Root, D. E.; Mino-Kenudson, M.; Brachtel, E. F.; Driggers, E. M.; Sabatini, D. M. *Nature* **2011**, *476*, 346.
- Fanga, H. Y.; Chen, S. B.; Guo, D. J.; Pan, S. Y.; Yu, Z. L. *Phytomedicine* **2011**, *18*, 697.
- Kusner, L. L.; Sarthy, V. P.; Mohr, S. *Invest. Ophthalmol. Vis. Sci.* **2004**, *45*, 1553.
- Ali, R. E.; Rattan, S. I. S. *Ann. N.Y. Acad. Sci.* **2006**, *1067*, 394.
- Mach, C. M.; Mathew, L.; Mosley, S. A.; Kurzrock, R.; Smith, J. A. *Anticancer Res.* **1995**, *2009*, 29.
- Yallapu, M. M.; Jaggi, M.; Chauhan, S. C. *Drug Discovery Today* **2012**, *17*, 71.
- Bourassa, P.; Kanakis, C. D.; Tarantilis, P.; Pollissiou, M. G.; Tajmir-Riahi, H. A. J. *Phys. Chem. B* **2010**, *114*, 3348.
- Chakraborti, S.; Das, L.; Kapoor, N.; Das, A.; Dwivedi, V.; Poddar, A.; Chakraborti, G.; Janik, M.; Basu, G.; Panda, D.; Chakraborti, P.; Suroliya, A.; Bhattacharyya, B. J. *Med. Chem.* **2011**, *54*, 6183.
- Gradis, H.; Keber, M. M.; Pristovs, P.; Jerala, R. *J. Leukocyte Biol.* **2007**, *82*, 968.
- Hafner-Bratkovic, I.; Gaspersic, J.; Smid, L. M.; Bresjanac, M.; Jerala, R. *J. Neurochem.* **2008**, *104*, 1553.
- Yang, F.; Lim, G. P.; Begum, A. N.; Ubada, O. J.; Simmons, M. R.; Ambegaokar, S. S.; Chen, P. P.; Kaye, R.; Glabe, C. G.; Frautschi, S. A.; Cole, G. M. *J. Biol. Chem.* **2005**, *280*, 5892.
- Daniel, S.; Limson, J. L.; Dairam, A.; Watkins, G. M.; Daya, S. J. *Inorg. Biochem.* **2004**, *98*, 266.
- Nafisi, S.; Adelzadeh, M.; Norouzi, Z.; Sarbolouki, M. N. *DNA Cell Biol.* **2009**, *28*, 201.
- Kurien, B. T.; Dillon, S. P.; Dorri, Y.; D'Souza, A.; Scofield, R. H. *Int. J. Cancer* **2011**, *128*, 239.